Forensic implications of novel synthesis of cathinone derivatives by Neber and modified Neber rearrangements

Forensic Chemistry 38 (2024) 100558

Contents lists available at ScienceDirect

Forensic Chemistry

journal homepage: www.sciencedirect.com/journal/forensic-chemistry

Forensic implications of novel synthesis of cathinone derivatives by Neber and modified Neber rearrangements

Cohan Huxley [a,c,d], Timothy J. Biddle [a], Ebony Shand [a,d], Wendy A. Loughlin [a,*], Sarah L. Cresswell [a], Urs D. Wermuth [a,b], Sue E. Boyd [a,c,d], Mark J. Coster [a,c,d]

[a] School of Environment and Science, Griffith University, Nathan, QLD 4111, Australia
[b] Forensic Sciences Queensland, 39 Kessels Rd, Coopers Plains, QLD 4108, Australia
[c] Griffith Institute for Drug Discovery, Griffith University, Brisbane, QLD 4111, Australia
[d] Retired, resigned, or no longer a student at Griffith University: Author credit attributed

ARTICLE INFO

Keywords:
Cathinone
Propiophenone
Route-specific markers
GC-EIMS
Density Functional Theory (DFT)

ABSTRACT

Cathinone and its synthetic analogues are known compounds of clandestine interest. Investigation into novel pathways for synthesising cathinone derivatives has potential for forensic analysis and tracking. The known Neber rearrangement of commercially available phenylpropanones that were evaluated yielded amides described herein and was not viable for clandestine synthesis of cathinone derivatives. Whereas the known modified Neber rearrangement of phenylpropanones that were evaluated via stable aziridine salts and subsequent treatment with acid, gave cathinone derivatives described herein in poor to low yields (2–17%). Assessment of the reagents, equipment, and procedures required for the modified Neber rearrangement was considered as only viable for more advanced clandestine operations. An improved understanding of the potential by-product formation from the modified Neber rearrangement was determined by density functional theory (DFT) of hydrazone to azirine to aziridine intermediates and attempted dynamic NMR spectroscopy of a hydrazone described herein. The substantially lower energy of the azirine step compared to the starting hydrazonium salt step of the reaction mechanism implied that the azirine structure was a short-lived intermediate, and unable to be experimentally determined. New mass-spectral fragmentation data of compounds described herein was reported, where differentiation was observed for some individual compounds at the GC-EIMS fragmentation pattern level. From this study, individual mass-spectrometry fragmentation of key compounds evaluated from the modified Neber rearrangement of commercially available phenylpropanones indicates potential for forensic profiling analysis applications.

1. Introduction

Amphetamine-type stimulants (ATS) are a class of illicit substance which pose a major public health concern [1]. ATS usage results in stimulation of the user's central nervous system and is accompanied with desirable effects including increased attentiveness and feelings of euphoria; the desirable effects render ATS addictive, but create health problems in the user and provide inherent dangers, through amphetamine psychosis, to both ATS users and the broader public [2,3]. There are many forms of ATS, including amphetamine, methamphetamine and a vast range of synthetic analogues and derivatives [1]. The weight of ATS seized worldwide has continued to increase, while the weight of ATS detected at the Australian border throughout 2018–2019 was the highest on record [1].

Many forms of ATS are routinely synthesised by clandestine laboratories [1]. Clandestine laboratories are illegally operating drug synthesis laboratories which pose a significant hazard to the public due to the chemicals used and produced [4]. Authorities use forensic signature profiling when investigating illicit drug seizures, and state-of the-art analytical approaches have been reviewed elsewhere [5]. Notably understanding and being able to identify the impurity signature profile of synthetic chemical agents provides a significant tool for authorities investigating illicit chemicals [6]. Importantly, constant changes in the synthetic patterns produce new impurity profiles, as illustrated in reviews of the clandestine sources of and new synthetic routes for methamphetamine. [7,8] Recently, a considerable proportion of clandestine

* Corresponding author.
E-mail address: w.loughlin@griffith.edu.au (W.A. Loughlin).

https://doi.org/10.1016/j.forc.2024.100558
Received 7 November 2023; Received in revised form 7 February 2024; Accepted 14 February 2024
Available online 17 February 2024

laboratories are reported to use mixed or unclassified methods of ATS production, circumventing the commonplace precursor chemicals in favour of less common synthetic pathways, which may not be known to authorities [9,10]. The latter development highlights the importance of investigations into synthetic pathways to ATS using precursors which are largely unregulated by authorities, to assist law enforcement and forensic services in tracking and preventing clandestine manufacture of ATS.

Since the early 2000's, trends in clandestine manufacture have demonstrated a marked shift towards production of synthetic analogues and derivatives of substances including ATS, which are commonly marketed and sold as 'designer drugs' or 'legal highs' [11,12]. Recently, authorities have detected cathinone derivatives both in Australia and worldwide [10,11,13]. Cathinones are broadly classified as phenethylamine derivatives with a β-keto moiety on the side chain and there are approximately 30 known cathinone derivatives, of which many have an amphetamine analogue, as related by reduction of the β-keto moiety (Fig. 1) [14]. Cathinone (2-amino-1-phenyl-1-propanone) **1** is the parent compound and exists in two enantiomer forms, with the (S)-(−)-enantiomer (Scheme 1) possessing the major pharmacological effects.

Cathinone **1** can be extracted from the leaves of the khat plant *Catha edulis* [15,16]. It has been observed that (S)-(−)-cathinone **1** can dimerise to produce the inactive product 3,6-dimethyl-2,5-diphenylpyrazine **2**, making it difficult to purify and isolate cathinone **1** (Scheme 1). However, cathinone **1**, as the free base, is stable in non-polar, non-hydroxylic solvent, such as dichloromethane [17]. Cathinone **1,** has a relatively simple structure which lends itself to accessible routes for clandestine manufacture [11] and consequently, research to improve the forensic understanding of routes for manufacturing cathinone **1** is of importance.

The traditional chemical precursor to cathinone **1** is α-bromophenyl-1-propanone (α-bromopropiophenone), which can be converted to racemic cathinone **1** through an S_N2 substitution reaction with ammonia. α-Bromopropiophenone can easily be produced from propiophenone through bromination under acidic conditions [18]. Additionally, (S)-(−)-cathinone **1** can be selectively synthesised. Resolution of norephedrine with *O*,*O*-dibenzoyl-*d*-tartaric acid, followed by conversion of the (S)-(−)-enantiomer to its *N*-formyl derivative, oxidation with chromium trioxide in pyridine and subsequent hydrolysis with hydrochloric acid gave (S)-(−)-cathinone **1** in moderate yield (39 %) [17].

Increased restrictions placed on the known reagents required for ATS production by authorities will continue to influence clandestine operators to shift toward novel manufacture routes [9]. A potentially viable, alternate method for the synthesis of cathinone **1** is using a Neber rearrangement, which was previously reported in older literature [19]. In the Neber rearrangement, the reaction of tosyl oxime of 1-phenyl-1-propanone (propiophenone) with base provided a 2H-azirine, which upon subsequent aqueous acid work-up was converted to an α-amino ketone [19] (Fig. 2, Y = Tos). In a 'modified Neber' rearrangement, reaction of quaternary hydrazones (Fig. 2, Y = NMe_3I) with bases provided 2H-azirines, which upon subsequent aqueous acid work-up formed α-amino ketones (Fig. 2), such as the hydrochloride salt of cathinone **1** [20]. The Neber rearrangement and the 'modified Neber' rearrangement have been reviewed elsewhere [21].

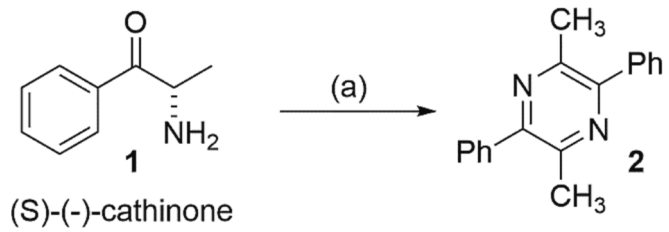

Scheme 1. Formation of diphenyl pyrazine **2**. *Reagents & Conditions:* (a) MeOH, 48 hr.

Currently, the mechanism for the Neber rearrangement is not established. The mechanism of the Neber rearrangement, including potential formation of an azirine intermediate in synthesis of cathinone **1** could be achieved using the newer techniques of dynamic nuclear magnetic resonance (NMR) experiments and density functional theory (DFT). Dynamic NMR is a technique used to possibly extract detailed mechanistic information inaccessible by other means [22]. In the present work, attempted dynamic NMR was conducted to physically measure the kinetics of the Neber rearrangement and the azirine intermediate in the synthesis of cathinone **1**. Complementary to dynamic NMR, DFT is an approach to modelling complex molecular systems, which has all but replaced wavefunction approaches in recent years, for the treatment of systems important to chemistry [23,24]. In the present work, DFT studies were conducted to evaluate the possibility for an azirine structure to exist as an intermediate within a proposed mechanism for the Neber rearrangement applied to the synthesis of cathinone **1**.

The aim of this study was to evaluate (1) the reported Neber rearrangement [19] and (2) subsequent modified Neber rearrangement reported by Sato [20] for the synthesis of cathinone **1** and simple derivatives, to provide an initial scope of the potential clandestine application of this synthetic approach. In addition, this study aimed to (3) gain a greater understanding of the viability of the synthetic routes including yields, ease of purification, and by-product formation, and aimed to (4) identify the potential application of mass-spectrometry identification of by-product route-specific markers for forensic analysis by authorities. The scope of the study included simple derivatives of cathinone **1**; compounds **3**–**5**, which were *para*-substituted with the fluoro, methoxy and methyl groups (Fig. 3). Support for the presence of an azirine structure as a stable intermediate in the mechanism of the modified Neber Reaction was examined through dynamic NMR

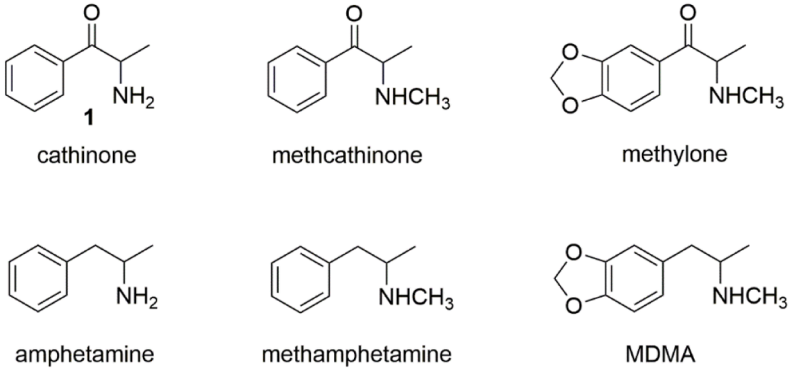

Fig. 1. Cathinone derivatives and their relationship to common ATS.

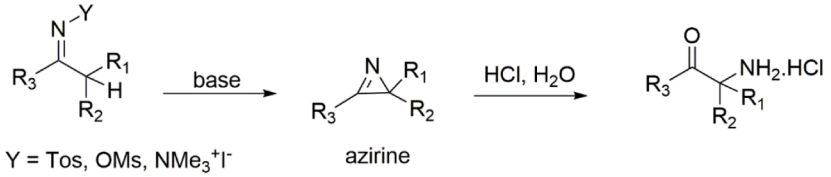

Fig. 2. Generalised steps for the Neber Rearrangement.

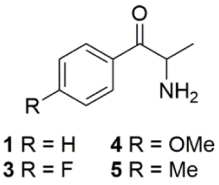

Fig. 3. Chemical structures of simple derivatives of cathinone **1**; hydrochloride salts **3**–**5**.

experiments and computational studies employing DFT. The potential for clandestine utilisation of the methodologies developed is discussed.

2. Materials and methods

2.1. Chemicals

Propiophenone (1-phenyl-1-propanone) **6** (Merck-Sigma-Aldrich), 4′-fluoropropiophenone **7** (Merck-Sigma-Aldrich), 4′-methoxypropiophenone **8** (Alfa Aesar), and 4′-methylpropiophenone **9** (Merck-Sigma-Aldrich), reagents such as *p*-toluenesulfonyl chloride (*p*-TosCl) (Alfa Aesar), 2-propanol (Fisher Chemicals), methyl iodide (Lancaster), acetic acid (BDH), formic acid (BDH), and solvents (VWR Chemicals) such as acetone and diethyl ether were obtained from commercial sources as indicated. All chemicals were purchased and used without purification.

2.2. Synthesis

2.2.1. Synthesis of oxime derivatives *10*–*14*

Aryl oxime derivatives were prepared from the appropriate propiophenone, hydroxylamine, and sodium hydroxide in ethanol, according to a literature method [25]. The resultant mixture was washed with DCM (30 mL, 3 × 10 mL). The organic layers were combined, and solvent removed *in vacuo*. The resulting oil was solubilised in 1:1 DCM: cyclohexane (20 mL) and solvent was removed *in vacuo* until a slurry was obtained. The product crystallised from the slurry after 16 h at 4 °C.

Propiophenone oxime **10**: Reaction of propiophenone **6** (2.97 g, 0.022 mol) according to the oxime derivative method gave propiophenone oxime **10** [26] as a solid (1.45 g, 44 %).

4-Fluoropropiophenone oxime **11**: Reaction of 4-fluoropropiophenone **7** according to the oxime derivative method gave 4-fluoropropiophenone oxime **11** as a solid (3.42 g, 0.022 mol). The resulting product was separated (24 g prepacked column; mobile phase: ethyl acetate/hexane; gradient: 100 % hexane to 80 % hexane over 20 mins). Product fractions were collected, and solvent was removed *in vacuo* yielding two yellow oils: 4-fluoropropiophenone oxime **11** [27] (0.82 g, 22 %) and 4-ethoxypropiophenone oxime **14** [28] (0.094 g, 2.2 %).

4-Methoxypropiophenone oxime **12**: Reaction of 4-methoxy propiophenone **8** (3.69 g, 0.023 mol) according to the oxime derivative method gave 4-methoxypropiophenone oxime **12** [29] as a white solid (1.92 g, 48 %).

4-Methylpropiophenone oxime **13**: Reaction of 4-methylpropiophenone **9** (3.24 g, 0.022 mol) according to the oxime derivative method gave 4-methylpropiophenone oxime **13** [30] as a white solid (1.92 g, 54 %).

2.2.2. Synthesis of amide derivatives *15*–*18*

Propiophenone oxime derivative **10**, **11**, **12** or **13** (~0.5 g) was added to a NaOH solution (2 M, 10 mL) and stirred for 10 mins. The reaction mixture was cooled to 0 °C while *p*-TosCl (0.65 g, 0.0034 mol) in acetone (5 mL) was added. The mixture was stirred for 1 h and water (0 °C, 40 mL) was added. The product was extracted in DCM (3 × 20 mL), and the organic layer dried (anhydrous Na_2SO_4) and solvent removed *in vacuo*. The resulting red oil was recrystallised in DCM/hexane and left at 4 °C for 16 h to afford crystals.

N-Phenylpropionamide **15**: Reaction of propiophenone oxime **10** (0.501 g, 0.0034 mol) according to the amide derivative method gave *N*-phenylpropionamide **15** [31–33] as a solid (0.073 g, 15 %).

N-(4-Fluorophenyl) propionamide **16**: Reaction of 4-fluoropropiophenone oxime **11** (0.62 g, 0.0037 mol) according to the amide derivative method gave a yellow oil determined to be 90 % pure by GC–MS. Purification by flash chromatography (24 g prepacked column; mobile phase: ethyl acetate/hexane; gradient: 70 % hexane to 50 % hexane over 20 min) gave *N*-(4-fluorophenyl) propionamide **16** [33,34] as a light brown oil (0.10 g, 19 %).

N-(4-Methoxyphenyl) propionamide **17**: Reaction of 4-methoxypropiophenone oxime **12** (0.59 g, 0.0033 mol) according to the amide derivative method gave a red oil. Extraction of the oil with diethyl ether, and recrystallisation (DCM/Hexane) gave *N*-(4-methoxyphenyl) propionamide **17** [33] as a solid (0.096 g, 16 %).

N-(4-Methylphenyl) propionamide **18**: Reaction of 4-methylypropiophenone oxime **13** (0.55 g, 0.0034 mol) according to the amide derivative method gave a red oil. Extraction of the oil with diethyl ether, and recrystallisation (chloroform) gave *N*-(4-methylphenyl) propionamide **18** [33,35] as a brown solid (0.23 g, 41 %).

2.2.3. Synthesis of hydrazone derivatives *19*–*22*

In an adaptation of a literature procedure [20], propiophenone **6**, **7**, **8**, or **9** (~3.3 g) was used as a solvent for the addition of 1,1-dimethylhydrazine (3.4 mL, 0.044 mol) to sodium acetate (0.27 g, 0.033 mol) and glacial acetic acid (~2 drops). The mixture was stirred and heated within a sealed tube for 16 h at 120 °C. The product as a yellow oil was extracted from the aqueous layer with diethyl ether (5 mL). The combined organic layers were washed with water (2 × 2 mL), dried (anhydrous Na_2SO_4) and the solvent removed *in vacuo*. Purification of the crude hydrazone via flash chromatography using the RediSep Flash Chromatogram system (24 g prepacked column; mobile phase: ethyl acetate/hexane; gradient: 100 % hexane to 80 % hexane over 20 min) and removal of the solvent removed *in vacuo* gave purified hydrazone.

1,1-Dimethyl-2-(1-phenylpropylidene)hydrazone **19**: Reaction of 1-phenylpropan-1-one **6** (3.0 g, 0.022 mol) according to the hydrazone derivative method, and purification gave 1,1-dimethyl-2-(1-phenylpropylidene)hydrazone **19** [36,37] as a yellow oil (2.79 g, 70 %).

2-[1-(4-Fluorophenyl)propylidene]-1,1-dimethylhydrazone **20**: Reaction of 4-fluoropropiophenone **7** (3.39 g, 0.022 mol). according to the hydrazone derivative method, and purification gave 2-[1-(4-fluorophenyl)propylidene]-1,1-dimethylhydrazone **20** as a yellow oil (2.34 g, 54 %). ^{1}H NMR (400 MHz, DMSO-d_6) δ 7.70–7.74 (m, 2H, H2′, H6′), 7.14–7.18 (m, 2H, H3′, H5′), 3.09 (q, J = 7.6 Hz, 2H, H2), 2.70 (s, 6H, H1″, H2″), 1.22 (3H, t, J = 7.7 Hz, H3); ^{13}C{^{1}H} NMR (100 MHz,

DMSO-d_6) δ 166.41 (C1), 162.49 (C4′, $^1J_{CF}$ = 246.6 Hz), 133.30 (C1′, $^4J_{CF}$ = 3.09 Hz), 128.81 (C2′, C6′, $^3J_{CF}$ = 8.3 Hz), 114.90 (C3′, C5′, $^2J_{CF}$ = 21.4 Hz) 47.49 (C1″, C2″), 20.52 (C2), 11.58 (C3); FTIR ν_{max}/cm^{-1}: 2952.8, 2855.7, 2772.7, 1690.5, 1602.1, 1507.4, 1463.8, 1222.3, 1156.8; TOF-HRMS**:** Calc. for $C_{11}H_{15}FN_2$ 195.1298 (M+H$^+$), Found 195.1403 (*m/z* M+H$^+$).

2-[1-(4-Methoxyphenyl)propylidene]-1,1-dimethylhydrazone **21**: Reaction of 4-methoxypropiophenone **8** (3.66 g, 0.022 mol) according to the hydrazone derivative method, and purification gave 2-[1-(4-methoxyphenyl)propylidene]-1,1-dimethylhydrazone **21** as a yellow oil (2.65 g, 58 %). ^{1}H NMR (400 MHz, DMSO-d_6) δ 7.88–7.90 (m, 2H, H2′, H6′), 7.13–7.15 (m, 2H, H3′, H5′), 3.99 (s, 3H, H1″), 3.04 (q, J = 7.7 Hz, 2H, H2), 2.66 (s, 6H, H1″, H2″), 1.22 (t, J = 7.6 Hz, 3H, H3); ^{13}C{^{1}H} NMR (100 MHz, DMSO-d_6) δ 167.10 (C1), 160.18 (C4′), 129.22 (C1′), 128.08 (C2′, C6′), 113.41 (C3′, C5′), 54.98 (C1‴), 47.58 (C1″, C2″), 20.34 (C2), 11.91 (C3); FTIR ν_{max}/cm^{-1}: 2950.6, 2851.8, 2769.9, 1681.0, 1600.1, 1509.5, 1246.6, 1172.7, 1031.5; TOF-HRMS: Calc. for $C_{12}H_{18}N_2O$ 207.1497 (M+H$^+$), Found 207.1614 (*m/z* M+H$^+$).

2-[1-(4-Methylphenyl)propylidene]-1,1-dimethylhydrazone **22**: Reaction of 4-methylpropiophenone **9** (3.26 g, 0.022 mol) according to the hydrazone derivative method, and purification gave 2-[1-(4-methylphenyl)propylidene]-1,1-dimethylhydrazone **22** as a yellow oil (2.94 g, 70 %). ^{1}H NMR (400 MHz, DMSO-d_6) δ 7.81–7.83 (m, 2H, H2′, H6′), 7.39–7.41 (m, 2H, 3H', H5′), 3.07 (q, J = 7.6 Hz, 2H, H2), 2.68 (s, 6H, H1″, H2″), 2.54 (s, 3H, H1‴), 1.22 (t, J = 7.7 Hz, 2H, 3H); ^{13}C{^{1}H} NMR (100 MHz, DMSO-d_6) δ 167.38 (C1), 138.29 (C1′), 134.11 (C4′), 128.64 (C2′, C6′), 126.60 (C3′, C5′), 47.55 (C1″, C2″), 20.70 (C1‴), 20.47 (C2), 11.79 (C3); FTIR ν_{max}/cm^{-1}: 2950.0, 2853.1, 2770.1, 1686.3, 1463.3, 1320.5, 1198.2; TOF-HRMS: Calc. for $C_{12}H_{18}N_2$ 191.1458 (M+H$^+$), Found 191.1657 (*m/z* M+H$^+$).

2.2.4. Synthesis of hydrazonium salt derivatives *23–26*

In an adaptation of a literature procedure [20], hydrazine **19, 20, 21** or **22** (~1.9 g) was added to an excess of methyl iodide (2.5 mL, 0.040 mol) and refluxed under inert atmosphere for 5 h at 60 °C. Diethyl ether (~5 mL) was added until a precipitate formed which was filtered and recrystallised (ethanol). The crystalline solid products were dried under vacuum.

2-(1-Phenylpropylidene)-1,1,1-trimethylhydrazon-1-ium iodide **23**: Reaction of 1,1-dimethyl-2-(1-phenylpropylidene)hydrazine **19** (1.76 g, 0.010 mol) according to the hydrazonium salt method gave 2-(1-phenylpropylidene)-1,1,1-trimethyl-hydrazon-1-ium iodide **23** [37] as white crystals (2.00 g, 63 %).

2-[1-(4-Fluorophenyl)propylidene]-1,1,1-trimethylhydrazonium iodide **24**: Reaction of 2-[1-(4-fluorophenyl)propylidene]-1,1-dimethylhydrazine **20** (1.94 g, 0.010 mol) according to the hydrazonium salt method gave 2-[1-(4-fluorophenyl)propylidene]-1,1,1-trimethylhydrazonium iodide **24** as a yellow crystalline solid (2.17 g, 65 %).^{1}H NMR (400 MHz, DMSO-d_6) δ 7.82–7.86 (m, 2H, H2′, H6′), 7.32–7.37 (m, 2H, H3′, H5′), 3.60 (s, 9H, H1″, H2″,H3″), 3.23 (q, J = 7.5 Hz, 2H, H2), 1.00 (t, J = 7.5 Hz, 3H, H3); ^{13}C{^{1}H} NMR (100 MHz, DMSO-d_6) δ 176.81 (C1), 163.97 (C4′, $^1J_{CF}$ = 249.83 Hz), 131.60 (C1′, $^4J_{CF}$ = 3.22 Hz), 130.67 (C2′, C6′, $^3J_{CF}$ = 9.01 Hz), 115.66 (C3′, C5′, $^2J_{CF}$ = 21.86), 56.74 (C1″, C2″, C3″), 24.28 (C2), 11.38 (C3); FTIR ν_{max}/cm^{-1}: 3034.6, 1601.4, 1509.3, 1310.9, 1224.4, 1166.9; TOF-HRMS: Calc. for $C_{12}H_{18}FN_2$ 209.1454 (M+H$^+$), Found 209.1581 (*m/z* M+H$^+$).

2-[1-(4-Methoxyphenyl)propylidene]-1,1,1-trimethylhydrazonium iodide **25**: Reaction of 2-[1-(4-methoxyphenyl)propylidene]-1,1-dimethylhydrazine **21** (2.061 g, 0.010 mol) according to the hydrazonium salt method gave 2-[1-(4-methoxyphenyl)propylidene]-1,1,1-trimethylhydrazonium iodide **25** as a white crystalline solid (1.76 g, 51 %). ^{1}H NMR (400 MHz, DMSO-d_6) δ 7.74–7.76 (m, 2H, H2′, H6′), 7.02–7.04 (m, 2H, H3′, H5′), 3.81 (s, 3H, H1‴), 3.58 (s, 9H, H1″, H2″, H3″), 3.19 (q, J = 7.5 Hz, 2H, H2), 1.03 (t, J = 7.4 Hz, 3H, H3); ^{13}C{^{1}H} NMR (100 MHz, DMSO-d_6) δ 176.58 (C1), 161.97 (C4′), 129.88 (C2′, C6′), 126.96 (C1′), 113.99 (C3′, C5′), 56.78 (C1″, C2″, C3″), 55.46 (C1‴), 23.67 (C2), 11.83 (C3); FTIR ν_{max}/cm^{-1}: 3493.8, 3433.5, 2971.4, 1592.0, 1513.0, 1257.6, 1177.4, 1016.0; TOF-HRMS: Calc. for $C_{13}H_{21}N_2O$ 221.1654 (M+H$^+$), Found 221.1787 (*m/z* M+H$^+$).

2-[1-(4-Methylphenyl)propylidene]-1,1,1-trimethylhydrazonium iodide **26**: Reaction of 2-[1-(4-methylphenyl)propylidene]-1,1-dimethylhydrazine **22** (1.90 g, 0.010 mol) according to the hydrazonium salt method gave 2-[1-(4-methylphenyl)propylidene]-1,1,1-trimethylhydrazonium iodide **26** as a white crystalline solid (1.01 g, 30 %). ^{1}H NMR (400 MHz, DMSO-d_6) δ 7.65–7.67 (m, 2H, H2′, H6′), 7.29–7.31 (m, 2H, H3′, H5′), 3.59 (s, 9H, H1″, H2″, H3″), 3.21 (q, J = 7.4 Hz, 2H, H2), 2.35 (s, 3H, H1‴), 1.00 (t, J = 7.4 Hz, 3H, H3); ^{13}C{^{1}H} NMR (100 MHz, DMSO-d_6) δ 177.49 (C1), 141.61 (C1′), 132.26 (C4′), 129.17 (C2′, C6′), 127.97 (C3′, C5′), 56.72 (C1″, C2″, C3″), 24.05 (C2), 20.88 (C1‴), 11.56 (C3); FTIR ν_{max}/cm^{-1}: 3028.2, 2997.1, 2946.1, 1602.6, 1462.8, 1306.8, 1241.2; TOF-HRMS: Calc. for $C_{13}H_{21}N_2$ 205.1705 (M+H$^+$), Found 205.1836 (*m/z* M+H$^+$).

2.2.5. Synthesis of cathinones *1, 3–5* and diphenyl pyrazine *2*

In an adaption of a literature method [20], hydrazonium iodide **23, 24, 25** or **26** (~1 g) was added to a solution of iPrONa in 2-propanol (1.8 M, 30 mL) and stirred at 40 °C for 16 h under an inert atmosphere. Removal of the solvent *in vacuo* afforded the crude product as a solid. The solid was extracted with hexane (2 × 20 mL). The combined organic layers were washed with thiosulfate solution (2 × 20 mL, 0.04 M), water (10 mL), dried (anhydrous Na_2SO_4) and the solvent removed *in vacuo*. The solid residue was dissolved in ether (20 mL) and hydrochloric acid (40 mL, 2 M). The solution was stirred at 0 °C for 30 min. The aqueous layer was washed with ether (2 × 10 mL) and removed *in vacuo*. The yellow/pink solid was left stand for 48hrs under light and washed with DCM until the washes showed no purple colour. The resulting solid was recrystallised from 2-propanol/ether.

2-Amino-1-phenyl-1-propanone hydrochloride **1**: Reaction of 1,1,1-trimethyl-2-(1-phenylpropylidene)-1,1,1-trimethylhydrazinium iodide **23** (1.01 g, 0.0032 mol) according to the cathinone method and purification gave 2-amino-1-phenyl-1-propanone hydrochloride **1** [38,39] as a white solid (0.102 g, 17 %).

2-Amino-1-(4-fluorophenyl)propanone hydrochloride **3**: Reaction of 2-[1-(4-fluorophenyl)propylidene]-1,1,1-trimethylhydrazinium iodide **24** (1.055 g, 0.0031 mol) according to the cathinone method and purification gave 2-amino-1-(4-fluorophenyl)propanone hydrochloride **3** [40] as a white solid (0.010 g, 2 %).

2-Amino-1-(4-methoxyphenyl)propanone hydrochloride **4**: Reaction of 2-[1-(4-methoxyphenyl)propylidene]-1,1,1-trimethylhydrazinium iodide **25** (1.096 g, 0.0031 mol) according to the cathinone method and purification gave 22-amino-1-(4-methoxyphenyl)propanone hydrochloride **4** [39,41] as a white solid 0.047 g, 7 %).

2-Amino-1-(4-methylphenyl)propanone hydrochloride **5**: Reaction of 2-[1-(4-methylphenyl)propylidene]-1,1,1-trimethylhydrazinium iodide **26** (0.914 g, 0.0028 mol) according to the cathinone method and purification gave 2-amino-1-(4-methylphenyl)propanone hydrochloride **5** [39,42], as a white solid (0.059 g, 11 %).

1,1-Trimethyl-2-(1-phenylpropylidene)hydrazin-1-ium iodide **23** (1.01 g, 0.0032 mol), potassium *tert*-butoxide (0.074 g, 0.66 mmol) and *tert*-butyl alcohol (3 mL) were heated at 50 °C for 90 mins. Removal of the solvent *in vacuo*, and extraction (hexane, 2 mL) gave an oil. GC–MS analysis indicated the presence of 3,6-dimethyl-2,5-diphenylpyrazine **2** [43] (60 %).

2.3. Fourier transform infrared (FTIR) spectroscopy

Infrared spectroscopy analysis was performed with a Thermo Nicolet 5700 FTIR spectrometer equipped with an attenuated total reflectance diamond cell, with 16 scans, from 4000 to 500 cm^{-1} at a resolution of 4.0 cm^{-1}. Spectra were acquired and processed using OMNIC version 7.3 software (Thermo Electron Corporation).

2.4. Mass spectrometry – (GC-EIMS; GC–MS; TOF-HRMS)

Gas chromatography-electron impact mass spectrometry (GC-EIMS) data and analyses for compounds **1**, **3**–**22** were performed using an Agilent HP-6890N Network GC System coupled to a HP-5975 mass spectrometer (Agilent HP-5MS capillary column, 30 m, 0.25 mm, 0.25 μm). Split injection (25.0:1) was used at a temperature of 100 °C. Typical GC oven temperature consisted of an initial temperature of 100 °C for 1 min raised to 280 °C at a ramp rate of 30 °C/min and held at 280 °C for 10 min. Ultra high purity helium (99.999 %) was used as the carrier gas, at a total flow rate of 1.0 mL/min.

Direct injection electrospray ionisation mass spectrometry (DI ESI-MS) analyses were performed for compounds **23**–**26** using a Water Micromass ZQ (100–700 (*m/z*); positive ion mode; source temperature: 100 °C; capillary voltage: 3.50 kV) coupled to a Waters Alliance 2695 Separation Module (isocratic; solvent: 5 % H_2O in methanol; flow rate: 1.0 mL/min) and processed using MassLynx 4.0 software. Semi-preparative high-performance liquid chromatography (HPLC) was conducted using a Shimadzu© LC-10ADVP instrument (Supelco Ascentis C18 column, 15 cm, 21.2 mm, 5 μm) and processed using Labsolutions software. Samples were loaded onto the column using an absorbent plug (constant flow rate: 5.0 mL/min) and gradient elution was used (5 % acetonitrile in H_2O to 25 % acetonitrile in H_2O over 15 min and held at 25 % for 5 min).

Accurate mass data was obtained using a PerkinElmer time of flight (TOF) mass spectrometer AxION 2 TOF (capillary entrance: 6000 V, endplate: 5000 V, cylinder: 3500 V; drying gas: 350 °C, 80 PSI at 14.0 L/min; mass range: 110–700 (*m/z*)). Samples were injected into an isocratic solvent stream delivered by a PerkinElmer Series 200 Pump (0.6 mL/min; 80:20 MeCN/Water, 0.1 % formic acid). IR data was attained on a Nicolet 5700 instrument and PerkinElmer FTIR Spectrometer Spectrum Two (default standard for analysing non-controlled and illicit substances with wavelengths ranging from 450 to 4000 cm^{-1}) and analysed using OMNIC (7.3) software for starting materials and Spectrum (10.03.09) software for major products.

GC-EIMS data obtained for compounds **1** and **6** were compared against available global MS library data from the National Institute of Standards and Technology (NIST): NIST14 Standard Reference Database. MS data for compounds **3**–**5**, **10**–**22** was not available in NIST14.

2.5. Nuclear magnetic resonance (NMR) spectroscopy

All nuclear magnetic resonance (NMR) spectra were acquired on a Bruker Avance Neo 400 MHz spectrometer in D_2O, DMSO-d_6 and $CDCl_3$ solvents at room temperature (300 K). ^1H and $^{13}C\{^1H\}$ NMR chemical shifts were referenced to solvent residuals, taken as: 4.80 ppm (D_2O), 2.49 ppm and 39.08 ppm (DMSO-d_6), 7.23 ppm and 77.0 ppm ($CDCl_3$) respectively. For the D_2O solvent system, sodium 2,2-dimethyl-2-silapentane-5-sulfonate (DSS) was used as an external reference, taken as: 0.00 ppm.

Attempted dynamic NMR spectroscopy of hydrazonium salt **25** (R = OMe): An iProNa solution (0.6 M) was prepared by dissolving sodium metal (92 mg) in isopropanol-d_8 (2 mL) under an inert atmosphere (N_2). Hydrazonium salt **25** (4.5 mg, ~0.013 mmol; obtained from 8.0 mg of recrystallised sample of **25** which contained 15 equivalents of water as determined by prior ^1H NMR spectroscopy) was added through a septum on an NMR tube to 550 μL of the *iso*-ProNa-d_7 solution (0.33 mmol *iso*-ProNa-d_7, 25 equivalents). DMSO-d_6 (100 μL) was added to aid solubility of hydrazonium salt **25**. The mixture was vortexed, and the reaction time recorded from this moment. The NMR tube was introduced to the NMR spectrometer and spectra were recorded at 298 K and at 5 min intervals for the first 15 min, after which the spectra were recorded at 30 min intervals for 3 h. Signals indicating the formation of isopropyl aziridine **31** were observed within t = 1.0 min of spectral acquisition.

2.8. Density function theory (DFT) analysis

The methodology employed for DFT analysis is analogous to previously reported methodology [44]. The molecular structures for all intermediates were produced and optimised using the universal force field (UFF) available in Avogadro 1.90.0 software [45]. These starting structures were subject to geometry optimisation at the ωB97X-D/6-311++G(d,p) level [46–48] using Gaussian 16 software (Wallingford, Connecticut, USA) [49] (Supporting Information) accessed through the [Griffith University] high-performance computing (HPC) cluster "[Gowanda]". This was followed by vibrational frequency analysis at the same level, ensuring convergence and no imaginary frequencies (Supporting Information).

3. Results and discussion

3.1. Neber rearrangement

In the present study, treatment of propiophenones **6**–**9** with hydroxylamine and sodium hydroxide, according to the initial Neber literature method [19], gave oxime derivatives **10**–**13**. Ethoxypropriophenoneoxime **14** was observed as a single by-product (<5% yield) of oxime **10** and was presumed to occur from nucleophilic aromatic substitution on the *para*-fluoro moiety of propiophenone **7**. Further, reaction of oximes **10**–**13** with sodium hydroxide followed by tosyl chloride failed to give the corresponding cathinone derivatives and instead formed the amides **15**–**18**, (Scheme 2), due to a Beckmann rearrangement. Modification of reaction conditions, with other bases/solvents such as sodium methoxide (NaOMe) in methanol, potassium ethoxide (KOEt) in ethanol and sodium hydride (NaH) in DMF or THF, also yielded the major products as the amides **15**–**18**. However, although use of potassium ethoxide as a base did provide small quantities of cathinone **1** (confirmed by GC–MS analysis), cathinone **1** proved difficult to isolate by standard laboratory procedures (i.e., flash chromatography with gradient elution). Furthermore, it is highly likely that the initial Neber literature method [19], due to the lack of analytical methods at the time, incorrectly identified cathinone **1** as the product. It was concluded that the initial Neber literature [19] approach to cathinone **1** was not viable for clandestine operations.

3.2. Modified Neber rearrangement

Attention was turned to a modified Neber rearrangement approach reported in the older literature [20], where rearrangement of hydrazonium salt **23** (R = H, Scheme 2) in the presence of potassium *tert*-butoxide/*tert*-butanol gave azirine **27**:propiophenone **6** (in a ratio of 55:45) and when excess sodium isopropoxide/isopropanol was used, aziridine **28** was formed (Fig. 4) [20]. Subsequent hydrolysis of aziridine **28** with hydrochloric acid was reported to give α-aminopropiophenone hydrochloride **1** (R = H, Scheme 2) [20].

Accordingly, treatment of *para*-substituted propiophenones **6**–**9** with 1,1-dimethylhydrazine (UDMH) gave hydrazone derivatives **19**–**22**. Subsequent treatment of hydrazone derivatives **19**–**22** with methyl iodide provided the target intermediates, hydrazonium salts **23**–**26** (Scheme 2), which were fully characterised by NMR spectroscopy, FTIR, GC–MS and TOF-HRMS.

However, treatment of **23** with excess potassium *tert*-butoxide using the modified Neber rearrangement procedure, unexpectedly provided the 3, 6-dimethyl-2,5-diphenylpyrazine **2** (ca. 60 % by GC–MS), arising from dimerization of cathinone **1**, presumably due to the presence of adventitious water (Scheme 3). Neither the azirine **27** nor cathinone **1**, were observed. Reaction of **23** with the alternate reagent, potassium *tert*-butoxide under anhydrous conditions, would be inaccessible to all but the most sophisticated clandestine laboratories; therefore, the reported procedure was not assessed further.

Instead, treatment of **23** with sodium isopropoxide (iPrONa) in

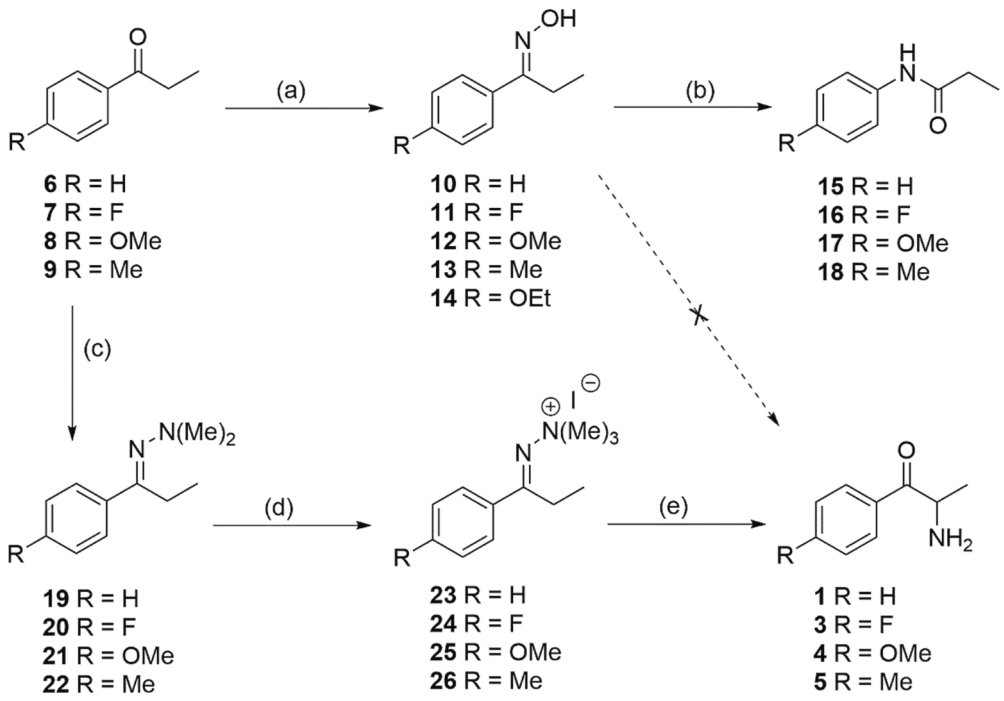

Scheme 2. Formation of amides **15**–**18** and cathinones **1**, **3**–**5**. *Reagents & Conditions:* (a) $HONH_2$.HCl, NaOH, EtOH, 90 °C, 1hr; (b) (i) NaOH (2 M), H_2O, 0 °C, 10 min, (ii) *p*-TosCl, acetone, 0 °C, 1 hr; (c) UDMH, cat. CH_3CO_2H, NaOAc, 120 °C, sealed tube, 16 hrs; (d) MeI, neat, 60 °C, 5hrs; (e) (i) excess *i*-PrONa, *i*-PrOH, 40 °C, 16hr; (ii) HCl (2 M), ether, 30 min.

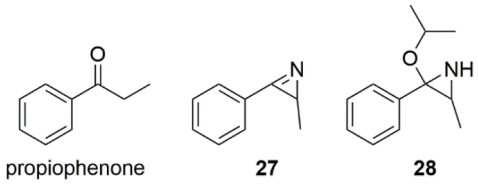

Fig. 4. Products from modified Neber rearrangement of 23, as reported in older literature [20].

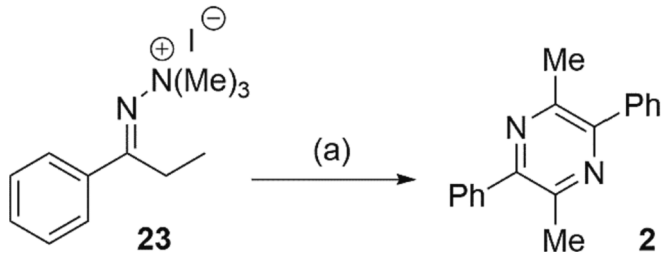

Scheme 3. Attempted modified rearrangement of propiophenone dimethyl hydrazone methiodide **23** *Reagents & Conditions:* (a) *t*-BuOK, *t*-BuOH, 50 °C, 1hr.

isopropanol according to the modified Neber rearrangement procedure reported by Sato [20], gave an intermediate, which was directly treated with hydrochloric acid to give the cathinone hydrochloride product **1**. Corresponding treatment of hydrazonium salts **24**, **25**, and **26** with excess sodium isopropoxide in isopropanol, then hydrochloric acid gave the cathinone hydrochloride products **3, 4** and **5** (Scheme 2). To avoid extensive cyclisation resulting in significant losses in yields, the cathinone products were purified to remove iodide-containing residues, followed by recrystallisation from isopropyl alcohol and diethyl ether [17] to obtain the stable cathinone derivatives **1**, **3**, **4** and **5**. This approach provided a viable synthesis of workable quantities of cathinone hydrochlorides **1**, **3**, **4** and **5**, which were analysed by GC-EIMS, FTIR, 1D and 2D NMR spectroscopy. Further analysis was carried out on mass spectral fragmentation of key intermediates and exploration of evidence for formation of azirine or aziridine intermediates.

3.3. Mass spectral fragmentation patterns

Identification of controlled substances in complex mixtures can be achieved using GC–MS analysis combined with a library search of reference standards [50]. However, impurity profiling may not have access to reference standards for each impurity. A search of the NIST14 database revealed that compounds **3**–**5** (cathinones), **10**–**14** (oximes), **15**–**18** (amides) and **19**–**22** (hydrazones) were not reported in the NIST14 database at the time of this research. The range of products and by-products (impurities) produced in this project, sought to profile possible impurities and/or synthetic intermediates, and add to the standards available for the identification of controlled substances. In particular, the value of mass-spectral fragmentation patterns adds to analysis and diagnosis by forensic services. For example, in the present study, oxime **13**, amide **18** and methyl cathinone **5** all have very similar (MH^+) parent ions of 164.1343, 164.1310 and 164.1329 respectively, which were obtained from TOF-HRMS experimental data. Notably, compounds **5**, **13** and **18** can be differentiated by characteristic fragmentation ions from GC-EIMS data (Table 1; experimental data). Oxime **13** has a peak at *m/z* at 146 (M-18; loss of water), amide **18** has fragmentation peaks at *m/z* at 107 (MH^+-$C(O)CH_2CH_3$) and at 57 ($CH_3CH_2CO^+$), and cathinone **5** has a fragmentation peak at *m/z* of 148 ($M–CH_3^+$). Mass spectral data and fragmentation patterns for compounds **1**, **3**–**5** (cathinones), **10**–**14** (oximes), **15**–**18** (amides) and **19**–**22** (hydrazones) were obtained from GC-EIMS and are reported in Supporting Information (Table S3.1) and add to the compounds available for identification by forensic services. Mass spectral data for the molecular ions of compounds **23**–**26** (hydrazonium salts) were obtained from ESI-MS, as these compounds were not suitable for GC-EIMS (Table S3.1).

Table 1
Accurate mass (TOF-MS) and mass spectral fragmentation patterns for compounds **5**, **13**, and **18**.

Compound number	Compound structure	Molecular Formula	HRMS ($M+H^+$)	GC-EIMS Fragmentation Ions
5	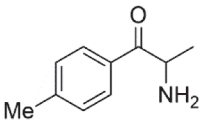	$C_{10}H_{13}NO$	164.1329	148, 132, 104, 91, 77
13	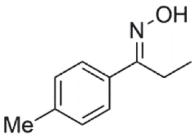	$C_{10}H_{13}NO$	164.1343	163, 146, 91
18	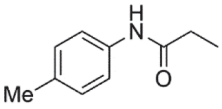	$C_{10}H_{13}NO$	164.1310	163, 107, 106, 57

3.4. NMR spectroscopy

Although, the evidence for the proposed mechanisms for the Neber rearrangement or substrate and condition variations, such as the modified Neber rearrangement [20], have been evaluated elsewhere [21], no conclusive mechanism has been established. Herein, we sought to explore whether an azirine intermediate could be observed to support a proposed mechanism for the Neber rearrangement and facilitate by-product profiling. During the synthetic studies (Scheme 2), NMR spectra were acquired directly on the crude intermediate isolated from treatment of hydrazonium salt **26** (R = Me) with excess sodium isopropoxide (iPrONa) in isopropanol, using the modified Neber rearrangement procedure [20]. ^{1}H, $^{13}C\{1H\}$, gCOSY, gHSQC and gHMBC NMR spectroscopic analysis gave evidence for isopropyl aziridine **29** being the major component of the crude intermediate (Scheme 4). Further details for evidence for isopropyl aziridine **29** are provided in the Supporting Information (Section 5).

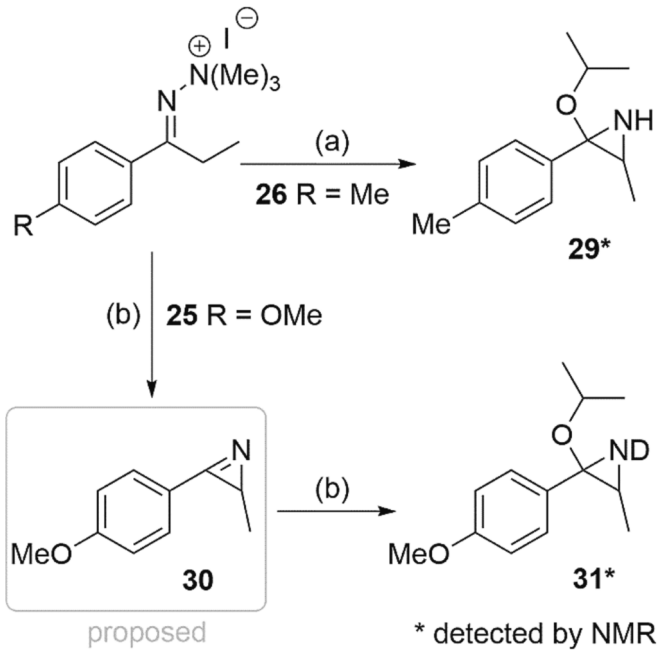

Scheme 4. Summary of NMR studies of attempted modified Neber rearrangement of propiophenone dimethyl hydrazone methiodides **25** (R = OMe) and **26** (R = Me). *Reagents & Conditions:* (a) excess *i*-PrONa, *i*-PrOH, 40 °C, 1hr; (b) *i*-PrONa-d_7, *i*-PrOH-d_8, 298 K.

Next, we sought to explore whether an azirine intermediate could be observed using dynamic NMR spectroscopy, and thus provide evidence supporting a stepwise mechanism. Methoxy-substituted hydrazonium salt **25** (R = OMe) was selected due to the presence of diagnostic signals in a simpler NMR spectrum, as compared to the other available hydrazonium salt derivatives.

Using the dynamic NMR spectroscopy protocol (Section 2.5) treatment of hydrazonium salt **25** (R = OMe) with deuterated sodium isopropoxide (i-ProNa-d_7) was monitored via NMR spectroscopy for 3 hrs at 298 K. The azirine intermediate **30** (Scheme 4) was not observed, and instead formation of aziridine **31** (Scheme 4) was observed within 15 min of monitoring. This established that azirine **30** (Scheme 4) was likely to be a very short-lived intermediate and thus conversion of hydrazonium salt **25** to azirine **30** or azirine **30** to aziridine **31** was unable to be observed by dynamic NMR spectroscopy at 298 K. The relatively high freezing point of the DMSO-d_6 (18.5 °C) or possible alternative solvents such as toluene-d_8, required to potentially solubilise the hydrazonium salt **25** mixture, made variable temperature NMR spectroscopy impractical for attempted resolution of the azirine intermediate **30** at lower temperature. It was decided that it was not worthwhile to pursue the NMR experiments further.

3.5. Density functional theory analysis

To further investigate whether the azirine species exists as a stable intermediate in the reaction mechanism, theoretical studies employing DFT were conducted. The ωB97X-D long-range corrected (LC) hybrid exchange–correlation (XC) functional was selected for this research due to its ability to model important chemical properties for a wide range of chemical species [46], combined with the 6–311++G(d,p) diffuse basis set [47,48]. Due to the requirement for modelling anionic species, a diffuse basis set was necessary in this research to obtain accurate results.

The complexity of the reaction system meant only the intermediates implicated in the proposed mechanism were investigated. For simplicity, the theoretical structures implicated in the proposed mechanism are labelled **A** through **F** (Fig. 5). The calculations employed the methoxide *para*-substituted structures since hydrazonium salt **25** (R = OMe) was utilised in the dynamic NMR experiments. Both the singlet

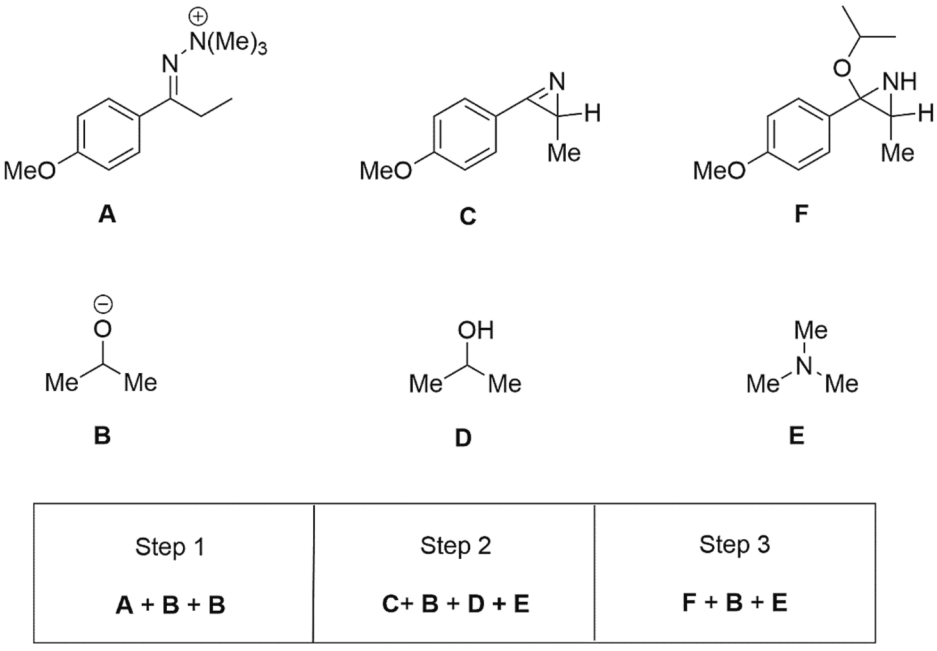

Fig. 5. Proposed participant species for the conversion of hydrazonium ion **A** (Step 1) to aziridine **F** (Step 3) through azirine intermediate **C** (Step 2).

and triplet multiplicities were trialled for each structure, and each were determined to be more stable in the singlet state (Supporting Information, Section 6). The sum of electronic and zero-point vibrational energy (E + ZPVE) values for each structure are annotated in Table 2. The combined E + ZPVE values (units: Ha) for the intermediates implicated in Step 1 to Step 3 are provided in Table 3 along with the E + ZPVE values relative to the initial Step 1 in units of Ha, kJ/mol and kcal/mol. The values were plotted in units of kJ/mol (Fig. 6).

Step 2, implicating azirine intermediate **C**, lies almost 548 kJ/mol lower in energy than Step 1 and over 72 kJ/mol higher in energy than Step 3. The placement of Step 2 between Step 1 and Step 3 may support the hypothesis that azirine intermediate **C** is a stable intermediate during the conversion of hydrazonium ion **A** to aziridine **F**. The considerable energetic advantage for the formation of azirine intermediate **C** implies that it would likely be a short-lived species in the mechanism, potentially rationalising the inability to observe this species during NMR experiments completed in this research.

4. Conclusions

The known Neber rearrangement [19] and modified Neber rearrangement [20] were evaluated as potential clandestine synthetic approaches to the amphetamine related compounds, cathinone **1** and cathinone derivatives. It was found that the Neber rearrangement of commercially available 1-phenylpropan-1-ones **6**–**9** by treatment with hydroxylamine/sodium hydroxide, followed by sodium hydroxide then tosyl chloride, did not yield cathinone derivatives **1**, **3**, **4**, and **5**, and instead yielded alternative products, amides **15**–**18**. The Neber rearrangement was not viable for clandestine syntheses. Whereas modified Neber rearrangement of commercially available 1-phenylpropan-1-ones **6**–**9** utilising iPrONa in isopropanol allowed the corresponding stable aziridine salts to be formed. Subsequently, *para*-substituted cathinone derivatives **1**, **3**, **4**, and **5** were obtained following addition of 2 M hydrochloric acid and were able to be purified through recrystallisation to obtain relatively low yields (2–17 %). Assessment of the reagents, equipment, and procedures required for the modified Neber rearrangement was considered as only viable for more advanced clandestine operations. An improved understanding of the potential by-product formation from the modified Neber rearrangement was determined by density functional theory (DFT) and attempted dynamic NMR spectroscopy.

Theoretical studies employing density functional theory (DFT) at the ωB97X-D/6-311++G(d,p) level demonstrated that the energy of the azirine structure lay between that of the hydrazonium salt and aziridine intermediates, supporting the potential of azirine as an intermediate in the proposed reaction mechanism for the modified Neber rearrangement [20]. The substantially lower energy of the azirine step compared to the starting hydrazonium salt step of the reaction mechanism implied that the azirine structure was a short-lived intermediate, rationalising the inability of the dynamic NMR experiments to observe azirine formation during the NMR scale reaction.

During the synthesis of cathinone derivatives **1**, **3**, **4**, and **5**,

Table 2
Energetics data obtained for the structures investigated in Fig. 5 calculated at the ωB97X-D/6-311++G(d,p) level. The values recorded reflect the singlet multiplicity for each structure, which was more stable in each case.

Structure	E (Ha)	ZPVE (Ha)	E + ZPVE (Ha)
A	−692.427	0.329	−692.098
C	−517.548	0.189	−517.359
F	−711.939	0.302	−711.637
B	−194.359	0.109	−193.649
D	−193.742	0.0928	−194.250
E	−174.467	0.121	−174.346

Table 3
Energetics data for the conversion of hydrazonium ion **A** (Step 1) to aziridine **F** (Step 3) implicating the azirine intermediate **C** (Step 2) (see Table 2) calculated at the ωB97X-D/6-311++G(d,p) level. The values recorded reflect the singlet multiplicity for each structure, which was more stable in each case. The E + ZPVE values for each species are recorded in units of Ha, kJ/mol and kcal/mol.

Structure	E + ZPVE (Ha)	Relative E + ZPVE (Ha)	Relative E + ZPVE (kJ/mol)	Relative E + ZPVE (kcal/mol)
Step 1 (**A** + **B** + **B**)	−1079.397	0	0	0
Step 2 (**B** + **C** + **D** + **E**)	−1079.605	−0.20863	−547.56	−130.87
Step 3 (**B** + **D** + **F**)	−1079.633	−0.23629	−620.17	−148.22

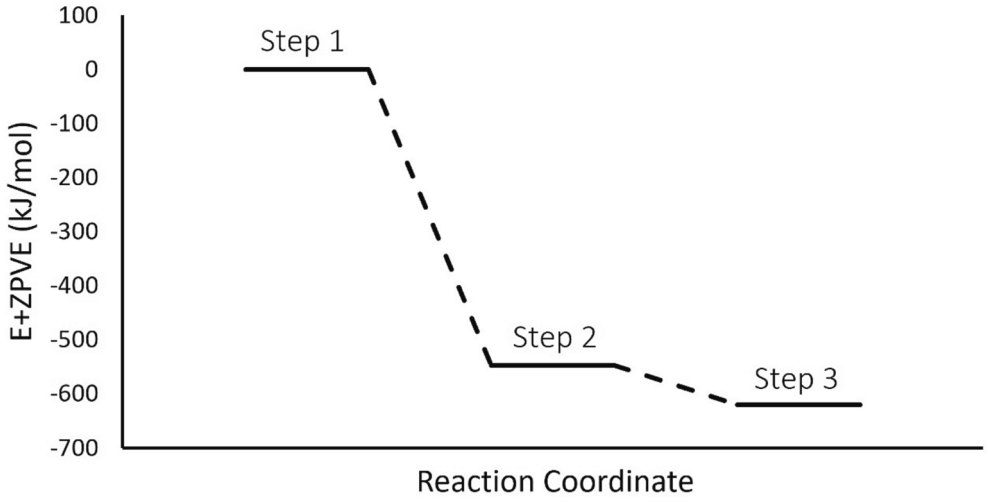

Fig. 6. Potential energy diagram for the three-step proposed mechanism for conversion of hydrazonium ion **A** to aziridine **F** through the azirine intermediate **C** (units: kJ/mol).

seventeen intermediate compounds and byproducts (compounds **1**, **3**–**5**, **10**–**26**) were isolated and spectral data acquired, including GC-EIMS. Several low intensity ions were related to the specific substitution patterns on the phenyl groups, and associated fragmentation of the side-chain of compounds (**1, 3**–**5, 10**–**22**). Despite compounds (**5, 13, 18**) having MH^+ parent ions within 0.003 amu, differentiation was observed at the individual compound GC-EIMS fragmentation pattern level. Identification of these by-products by mass-spectrometry fragmentation indicates the potential for forensic profiling analysis applications.

CRediT authorship contribution statement

Cohan Huxley: Formal analysis, Investigation, Validation. **Timothy J. Biddle:** Formal analysis, Investigation, Software, Validation, Writing – original draft, Writing – review & editing. **Ebony Shand:** Formal analysis, Investigation. **Wendy A. Loughlin:** Formal analysis, Writing – original draft, Writing – review & editing. **Sarah L. Cresswell:** Methodology, Supervision, Writing – review & editing. **Urs D. Wermuth:** Conceptualization, Methodology, Resources, Supervision, Writing – review & editing. **Sue E. Boyd:** Formal analysis, Methodology, Supervision. **Mark J. Coster:** Methodology, Supervision.

Declaration of competing interest

The authors declare that they have no known competing financial interests or personal relationships that could have appeared to influence the work reported in this paper.

Data availability

The authors do not have permission to share data.

Acknowledgments

This work was supported by Queensland Health Forensic and Scientific Services and Griffith University, including access to the Griffith University High-Performance Computing Cluster ‘Gowonda’.

Appendix A. Supplementary data

Supplementary data to this article can be found online at https://doi.org/10.1016/j.forc.2024.100558.

References

[1] Australian Criminal Intelligence Commission, Illicit Drug Data Report 2018-2019. https://www.acic.gov.au/sites/default/files/2020-09/illicit_drug_data_report_2018-19_internals_v10_introduction_ch.pdf, 2020 (acessed 11 September 2023).
[2] W.J. Panenka, R.M. Procyshyn, T. Lecomte, G.W. Macewan, S.W. Flynn, W. G. Honer, A.M. Barr, Methamphetamine use: A comprehensive review of molecular, preclinical and clinical findings, Drug Alcohol Depend. 129 (2013) 167–179, https://doi.org/10.1016/j.drugalcdep.2012.11.016.
[3] D. Ciccarone, Stimulant abuse: pharmacology, cocaine, methamphetamine, treatment, attempts at pharmacotherapy, Prim. Care 38 (2011) 41–58, https://doi.org/10.1016/j.pop.2010.11.004.
[4] J. Wright, J. Edwards, S. Walker, Exposures associated with clandestine methamphetamine drug laboratories in Australia, Rev. Environ. Health 31 (2016) 329–352, https://doi.org/10.1515/reveh-2016-0017.
[5] R. Ahmed, M.J. Altamimi, M. Hachem, State-of-the-art analytical approaches for illicit drug profiling in forensic investigations, Molecules 27 (6602) (2022) 1–16, https://doi.org/10.3390/molecules27196602.
[6] S.P.B. Ovenden, L.J. McDowall, H.E. McKeown, N.W. McGill, O.A.H. Jones, J. R. Pearson, M. Petricevic, M.L. Rogers, T.J. Rook, J. Williams, R.L. Webster, S. D. Zanatta, Investigating the chemical impurity profiles of fentanyl preparations and precursors to identify chemical attribution signatures for synthetic method attribution, Forensic Sci. Int. 321 (110742) (2021) 1–11, https://doi.org/10.1016/j.forsciint.2021.110742.
[7] I. Onoka, A.T. Banyika, P.N. Banerjee, J.J. Makangara, L. Dujourdy, A review of the newly identified impurity profiles in methamphetamine seizures, Forensic Sci. Int.: Synergy 2 (2020) 194–205, https://doi.org/10.1016/j.fsisyn.2020.06.004.
[8] S.G. Toske, T.D. McKibben, Monitoring methamphetamine in the United States: a two-decade review as seen by the DEA methamphetamine profiling program, Drug Test. Anal. 14 (2022) 416–426, https://doi.org/10.1002/dta.3186.
[9] J.K. Cunningham, J.C. Maxwell, M. Campollo, L.M. Liu, W.J. Lattyak, R. C. Callaghan, Mexico’s precursor chemical controls: Emergence of less potent types of methamphetamine in the United States, Drug Alcohol Dependence. 129 (2013) 125–136, https://doi.org/10.1016/j.drugalcdep.2012.10.001.
[10] Australian Crime Commission, Illicit Drug Data Report 2015-2016, https://www.acic.gov.au/sites/default/files/2020-08/illicit_drug_data_report_2015-16_full_report.pdf 2017 (acessed 11 September 2023).
[11] M.J. Valente, P.G. de Pinho, M.L. de Bastos, F. Carvalho, M. Carvalho, Khat and synthetic cathinones: A review, Arch. Toxicol. 88 (2014) 15–45, https://doi.org/10.1007/s00204-013-1163-9.
[12] S.D. Brandt, L.A. King, M. Evans-Brown, The new drug phenomenon, Drug Test. Anal. 6 (2014) 587–597, https://doi.org/10.1002/dta.1686.
[13] W. Abebe, Khat and synthetic cathinones: Emerging drugs of abuse with dental implications, Oral Surg. Oral Med. Oral Pathol. Oral Radiol. 125 (2018) 140–146, https://doi.org/10.1016/j.oooo.2017.11.015.
[14] J.P. Kelly, Cathinone derivatives: a review of their chemistry, pharmacology and toxicology, Drug Test. Anal. 3 (2011) 439–453, https://doi.org/10.1002/dta.313.
[15] S. Geisshusler, R. Brenneisen, The content of psychoactive phenylpropyl and phenylpentenyl khatamines in Catha edulis Forsk. of different origin, J. Ethnopharmacol. 19 (1987) 269–277, https://doi.org/10.1016/0378-8741(87)90004-3.
[16] R. Brenneisen, H.-U. Fisch, U. Loelbing, S. Geisshusler, P. Kalix, Amphetamine-like effects in humans of the khat alkaloid cathinone, Br. J. Clin. Pharmacol. 30 (1990) 825–882, https://doi.org/10.1111/j.1365-2125.1990.tb05447.x.
[17] B.D. Berrang, A.H. Lewin, F.I. Carroll, Enantiomeric α-aminopropiophenones (Cathinone): Preparation and investigation, J. Org. Chem. 47 (1982) 2643–2647, https://doi.org/10.1021/jo00134a026.

[18] M. Collins, A. Doddridge, H. Salouros, Cathinones: Isotopic profiling as an aid to linking seizures, Drug Test. Anal. 8 (2015) 903–909, https://doi.org/10.1002/dta.1886.
[19] P.W. Neber, G. Huh, Eine Neue, Allgemeine Methode Zur Gewinnung von α-aminoketonen. I, Justus Liebigs Ann. Chem. 515 (1935) 283–296, https://doi.org/10.1002/jlac.19355150119.
[20] S. Sato, I.I.I. Azirines, The preparation of azirine derivatives by the base-catalyzed rearrangement of quaternary hydrazones, Bull. Chem. Soc. Jpn 41 (1968) 1440–1444, https://doi.org/10.1246/bcsj.41.1440.
[21] W.F. Berkowitz, The Neber Rearrangement, Organic Reactions, Wiley and Sons, 2012, pp. 321–410, https://doi.org/10.1002/0471264180.or078.02.
[22] G. Binsch, H. Kessler, The kinetic and mechanistic evaluation of NMR spectra. New analytical methods (18), Angew. Chem. Int. Ed. Engl. 19 (1980) 411–428, https://doi.org/10.1002/anie.198004113.
[23] T. Schwabe, S. Grimme, Theoretical thermodynamics for large molecules: Walking the thin line between accuracy and computational cost, Acc. Chem. Res. 41 (2008) 569–679, https://doi.org/10.1021/ar700208h.
[24] S. Geerlings, S. Fias, Z. Boisdenghien, F.D. Proft, Conceptual DFT: Chemistry from the linear response function, Chem. Soc. Rev. 43 (2014) 4989–5008, https://doi.org/10.1039/C3CS60456J.
[25] K.N. Campbell, J.F. McKenna, The action of Grignard reagents on oximes. I. The action of phenylmagnesium bromide on mixed ketoximes, J. Org. Chem. 4 (1939) 198–205, https://doi.org/10.1021/jo01214a012.
[26] H. Zhao, C.P. Vandenbossche, S.G. Koenig, S.P. Singh, R.P. Bakale, An efficient synthesis of enamides from ketone, Org. Lett. 10 (2008) 505–507, https://doi.org/10.1002/chin.200827068.
[27] CAS Reference Number: 844470-85-5, Commercially available.
[28] CAS Reference Number: 91247-25-5, Commercially available.
[29] T.W.J. Taylor, CCLXXII. The configurations of the α-oximinoketones, J. Chem. Soc. (1931) 2018–2027, https://doi.org/10.1039/jr9310002018.
[30] CAS Reference Number: 59507-21-0, Commercially available.
[31] P. Metz, C. Mues, Thermal o→ c rearrangement of n-phenyl allylimidates, Tetrahedron 44 (1988) 6841–6853, https://doi.org/10.1016/s0040-4020(01)86212-8.
[32] H. Eshghi, Z. Gordi, An easy method for the generation of amides from ketones by a Beckmann type rearrangement mediated by microwave, Synth. Commun. 33 (2003) 2971–2978, https://doi.org/10.1081/scc-120022469.
[33] C. Ramalingan, Y.T. Park, Mercury-catalyzed rearrangement of ketoximes into amides and lactams in acetonitrile, J. Org. Chem. 12 (2007) 4536–4538, https://doi.org/10.1021/jo070297k.
[34] S. Naik, G. Bhattacharjya, B. Talukdar, B.K. Patel, Chemoselective acylation of amines in aqueous media, Eur. J. Org. Chem. 6 (2004) 1254–1260, https://doi.org/10.1002/ejoc.200300620.
[35] X. Li, Y. Zhang, Facile preparation of amides from azo compounds by SmI_2, Indian J. Chem. Sect. 45 (2006) 1576–1578, https://doi.org/10.1002/chin.200640079.
[36] A. Padwa, T.J. Blacklock, P.H.J. Carlsen, M. Pulwer, Synthetic approaches toward the bi (2H-azirine) system, J. Org. Chem. 44 (1979) 3281–3287, https://doi.org/10.1021/jo01333a001.
[37] G.R. Newkome, D.L. Fishel, Pyrolysis of ketone N, N, N-trimethylhydrazonium fluoroborates. Evidence for the genesis of pyridines, J. Org. Chem. 37 (1972) 1329–1336, https://doi.org/10.1021/jo00974a011.
[38] K. Koga, K. Yamada, X. Stereochemical Studies, Effects of neighboring functional groups on 1, 2-asymmetric induction in the reduction of propiophenone derivatives with sodium borohydride, Chem. Pharm. Bull. 20 (1972) 526–538, https://doi.org/10.1248/cpb.20.526.
[39] M. Osorio-Olivares, M.C. Rezende, S. Sepúlveda-Boza, B.K. Cassels, A. Fierro, MAO inhibition by arylisopropylamines: The effect of oxygen substituents at the β-position, Bioorg. Med. Chem. 12 (2004) 4055–4066, https://doi.org/10.1016/j.bmc.2004.05.033.
[40] J. Ermert, K. Hamacher, H.H. Coenen, N.C.A. ^{18}F-labelled norephedrine derivatives via α-aminopropiophenones, J. Labelled Compd. Radiopharm. 43(14) (2000) 1345-1363. https://doi.org/10.1002/1099-1344(200012)43:14<1345::aid-jlcr424>3.0.co;2-n.
[41] W.H. Hartung, J.C. Munch, E. Miller, F. Crossley, Amino alcohols. VII. Phenolic arylpropanolamines, J. Am. Chem. Soc. 53 (1931) 4149–4160, https://doi.org/10.1021/ja01362a033.
[42] J. Nyitrai, R. Markovits-Kornis, K. Lempert, Hydantoins, thiohydantoins and glycocyamidines. 27. Reductive rearrangements of retrobenzilic acid type induced by Lewis acids. 4. Scope of aluminium chloride induced reactions of dithiohydantoins with arenes, Acta Chim. Acad. Sci. Hung. 60 (1969) 141.
[43] A. Vidal-Albalat, S. Rodriguez, F.V. Gonzalez, Nitroepoxides as versatile precursors to 1,4-diamino heterocycles, Org. Lett. 16 (2014) 1752–1755, https://doi.org/10.1021/ol500444z.
[44] T.J. Biddle, U.D. Wermuth, W.A. Loughlin, S.L. Cresswell, A.R. White, Potential forensic markers from synthetic pathways to 1-phenyl-2-propanone from uncontrolled and controlled substances, Forensic Chem. 28 (2022) 100410, https://doi.org/10.1016/j.forc.2022.100410.
[45] M.D. Hanwell, D.E. Curtis, D.C. Lonie, T. Vandermeersch, E. Zurek, G.R. Hutchison, Avogadro: An advanced semantic chemical editor, visualization, and analysis platform, J. Cheminf. 4 (2012) 1–17, https://doi.org/10.1186/1758-2946-4-17.
[46] J.-D. Chai, M. Head-Gordon, Long-range corrected hybrid density functionals with damped atom–atom dispersion corrections, Phys. Chem. Chem. Phys. 10 (2008) 6615–6620, https://doi.org/10.1039/B810189B.
[47] M.J. Frisch, J.A. Pople, J.S. Binkley, Self-consistent molecular orbital methods 25. Supplementary functions for Gaussian basis sets, J. Chem. Phys. 80(7) (1984) 3265-3269, https://doi.org/10.1063/1.447079.
[48] J.A. Pople, D.L. Beveridge, Approximate Molecular Orbital Theory, McGraw-Hill, New York, 1970.
[49] M.J. Frisch, G.W. Trucks, H.B. Schlegel, G.E. Scuseria, M.A. Robb, J.R. Cheeseman, G. Scalmani, V. Barone, G.A. Petersson, H. Nakatsuji, X. Li, M. Caricato, A. V. Marenich, J. Bloino, B.G. Janesko, R. Gomperts, B. Mennucci, H.P. Hratchian, J. V. Ortiz, A.F. Izmaylov, J.L. Sonnenberg, D. Williams-Young, F. Ding, F. Lipparini, F. Egidi, J. Goings, B. Peng, A. Petrone, T. Henderson, D. Ranasinghe, V. G. Zakrzewski, J. Gao, N. Rega, G. Zheng, W. Liang, M. Hada, M. Ehara, K. Toyota, R. Fukuda, J. Hasegawa, M. Ishida, T. Nakajima, Y. Honda, O. Kitao, H. Nakai, T. Vreven, K. Throssell, J.A. Montgomery Jr., J.E. Peralta, F. Ogliaro, M. J. Bearpark, J.J. Heyd, E.N. Brothers, K.N. Kudin, V.N. Staroverov, T.A. Keith, R. Kobayashi, J. Normand, K. Raghavachari, A.P. Rendell, J.C. Burant, S.S. Iyengar, J. Tomasi, M. Cossi, J.M. Millam, M. Klene, C. Adamo, R. Cammi, J.W. Ochterski, R.L. Martin, K. Morokuma, O. Farkas, J.B. Foresman, D.J. Fox, Gaussian 16, Revision C.01, Gaussian Inc, Wallingford CT, 2019.
[50] S. Stein, Mass spectral reference libraries: an ever-expanding resource for chemical identification, Anal. Chem. 84 (2012) 7274–7282, https://doi.org/10.1021/ac301205z.